

Interaction of Pyrimethamine, Cycloguanil, WR99210 and their Analogues with *Plasmodium falciparum* Dihydrofolate Reductase: Structural Basis of Antifolate Resistance

Giulio Rastelli,^a Worachart Sirawaraporn,^{b,*} Pornthep Sompornpisut,^c Tirayut Vilaivan,^c Sumalee Kamchonwongpaisan,^d Rachel Quarrell,^e Gordon Lowe,^e Yodhathai Thebtaranonth^f and Yongyuth Yuthavong^d

^aDipartimento di Scienze Farmaceutiche, Università di Modena e Reggio Emilia, Via Campi, 183-41100 Modena, Italy

^bDepartment of Biochemistry, Faculty of Science, Mahidol University, Bangkok 10400, Thailand

^cDepartment of Chemistry, Faculty of Science, Chulalongkorn University, Bangkok 10330, Thailand

^dNational Center for Genetic Engineering and Biotechnology, National Science and Technology Development Agency, Bangkok 10400, Thailand

^eDyson Perrins Laboratory, South Parks Road, Oxford University, Oxford OX1 3QY, UK

^fDepartment of Chemistry, Faculty of Science, Mahidol University, Bangkok 10400, Thailand

Received 29 October 1999; accepted 15 January 2000

Abstract—The nature of the interactions between *Plasmodium falciparum* dihydrofolate reductase (pfDHFR) and antimalarial antifolates, i.e., pyrimethamine (Pyr), cycloguanil (Cyc) and WR99210 including some of their analogues, was investigated by molecular modeling in conjunction with the determination of the inhibition constants (K_i). A three-dimensional structural model of pfDHFR was constructed using multiple sequence alignment and homology modeling procedures, followed by extensive molecular dynamics calculations. Mutations at amino acid residues 16 and 108 known to be associated with antifolate resistance were introduced into the structure, and the interactions of the inhibitors with the enzymes were assessed by docking and molecular dynamics for both wild-type and mutant DHFRs. The K_i values of a number of analogues tested support the validity of the model. A ‘steric constraint’ hypothesis is proposed to explain the structural basis of the antifolate resistance. © 2000 Elsevier Science Ltd. All rights reserved.

Introduction

The dihydrofolate reductase (DHFR) domain of *Plasmodium falciparum* bifunctional dihydrofolate reductase-thymidylate synthase (DHFR-TS) is one of the few well-defined targets in malarial chemotherapy. The enzyme catalyzes the nicotinamide adenine dinucleotide phosphate (NADPH) dependent reduction of dihydrofolate to tetrahydrofolate. DHFR has received considerable attention as it is the target of pyrimethamine

(Pyr) and cycloguanil (Cyc) and other antifolates used for prophylaxis and treatment of *P. falciparum* infection. The rapid emergence of antifolate resistant *P. falciparum* has unfortunately compromised the clinical utilities of the drugs, and thus highlights the urgent need to search for new effective antifolate antimalarials.

Analysis of the gene encoding DHFR from *P. falciparum* parasites obtained from geographically distant sources and with different degrees of resistance suggested the association of antifolate resistance with point mutations of the gene coding for *P. falciparum* DHFR.^{1–9} Mutations of one or more residues at amino acid positions 16, 51, 59, 108, and 164 of the *P. falciparum* DHFR were identified to be involved in antifolate resistance. Evidence available recently also supports the hypothesis that antifolate resistance in malaria evolved in a step-wise selection of mutants, with multiple mutations subsequent to a single S108N mutation, and that

Abbreviations: Cyc, cycloguanil; Pyr, pyrimethamine; pfDHFR, *Plasmodium falciparum* dihydrofolate reductase; RMS, root mean square; TES, *N*-tris (hydroxymethyl)-methyl-2-aminoethane-sulfonic acid; H₂folate, 7,8-dihydrofolate; fs, femto-second; RESP, restrained electrostatic potential.

*Corresponding author. Tel.: +662-245-5195; fax: +662-248-0375; e-mail: scwsr@mahidol.ac.th

mutants which do not survive in nature were either poorly resistant to the drugs or had insufficient catalytic activity of DHFR to support DNA synthesis.¹⁰

While the parasites with A16V+S108T double mutation in the *dhfr* gene are resistant to Cyc but susceptible to Pyr, those with cross resistance to both drugs have either single or multiple mutations at amino acid residues 51, 59, 108 and 164.^{5–7,11} Since the structures of Pyr and Cyc are very closely similar, the questions arise as to why Cyc-resistant but Pyr-sensitive evolved while the reverse has never been reported in the natural isolates, and whether the binding of Pyr and Cyc to the wild-type and the mutant DHFRs are different. Similar questions can also be raised with WR99210, a dihydro-triazine whose structure is closely related to Cyc. The fact that WR99210 is highly effective against both Pyr-sensitive and -resistant parasites in vivo¹² and the DHFRs in vitro¹³ has made WR99210 an attractive compound for further studies.

In order to address the problems of binding modes of Pyr, Cyc, and WR99210, structural data of *P. falciparum* DHFR are needed. In the absence of pfDHFR structure from X-ray diffraction analysis, it is necessary to construct and predict the structure of the enzyme by a homology modeling approach.¹⁴ Such modeling approach has been exploited for the prediction of the structure of the new drug leads capable of inhibiting *P. falciparum* DHFR at micromolar and submicromolar levels.¹⁵ Using the model built from the 3D-structure of *Leishmania major* DHFR-TS, McKie et al.¹⁶ predicted that the S108N mutation of the *P. falciparum* DHFR would lead to a steric clash with the *p*-Cl atom of Pyr. The hypothesis was readily tested by modifying the Pyr structure to avoid the steric constraint, hence resulting in two Pyr analogues which are highly effective against Pyr-resistant DHFR and malarial parasites.¹⁶ Indeed, through analysis of a number of physicochemical characteristics of residues at position 108 of *P. falciparum* DHFR and compared with their activities against a series of drugs including Pyr, Cyc, TMP (trimethoprim), and WR99210, Warhurst has recently pointed out that mutant DHFRs with bulky groups at residue 108 would cause steric constraint and hence result in poor binding with the inhibitor.¹⁷

In this paper, we describe the construction of a homology model of DHFR domain of the bifunctional *P. falciparum* DHFR-TS, and the structures of the complexes between Pyr, Cyc and WR99210 with the wild-type, A16V, S108T, and A16V+S108T mutant enzymes. We predict from the model that A16V mutation of *P. falciparum* DHFR imposes a steric conflict for binding to Cyc as opposed to Pyr and WR99210, and that the steric conflict becomes more pronounced when combined with mutation at residue 108 in the A16V+S108T double mutants. The hypothesis was tested against experimental data on the binding strengths of analogues of these drugs to both wild-type and mutant enzymes. This model was used to design and synthesize new compounds which were tested against wild-type and resistant *P. falciparum* in vitro.

Materials and Methods

Homology modeling of *Plasmodium falciparum* DHFR

The structure of the DHFR domain of *P. falciparum* bifunctional DHFR-TS was obtained from homology modeling simulations. The model was constructed by alignment of *P. falciparum* DHFR primary sequence¹⁸ with the DHFR sequences of which the crystal structures are already known; these include DHFRs from *Escherichia coli*,¹⁹ *Lactobacillus casei*,²⁰ human,^{21,22} chicken liver²³ and *Pneumocystis carinii*.²⁴ Unfortunately, the *Leishmania major* bifunctional DHFR-TS was not included into the sequence alignment as the crystal structure was not publicly available at the time the model was built. The alignment of *P. falciparum* DHFR sequence¹⁸ was carefully checked by using the available sequence alignment evaluation functions within MODELLER 3.0,²⁵ and by superimposing the structurally conserved regions of the available DHFR crystal structures.

The model of pfDHFR was constructed using MODELLER 3.0.²⁵ A primary homology model was constructed based on the conserved regions of most DHFRs by removing the sequences of the two insertions, i.e., residues 22–38 and 64–98. Next, several models were constructed on the whole sequence by adding one at a time the local alignments found to fill the two insertions. Local alignments were predicted using BLAST (Basic Local Alignment Search Tool)²⁶ at the National Center for Biotechnology Information, NCBI (web site hyperlink <http://www.ncbi.nlm.nih.gov/blast>). A stringent significant threshold of 3 was adopted for the BLAST search. Then, combinations of these, and finally all the local alignments were introduced. The model showing the best score as judged by the value of the Modeller objective function, and with the least root mean square (RMS) deviation with respect to the conserved regions of the DHFR templates, was saved for further refinement with molecular dynamics. The quality of the stereochemistry and of the structures was validated using the PROCHECK²⁷ and WHATIF tools available at the Biotech Validation Suite for Protein Structures (web site <http://biotech.embl-heidelberg.de:8400/>).

Molecular dynamics refinement of the structure

The pfDHFR structure resulting from MODELLER was refined by means of molecular mechanics and molecular dynamics calculations using AMBER 4.1²⁸ and the all-atom force field by Cornell et al.²⁹ Bond lengths involving hydrogens were constrained using the SHAKE algorithm³⁰ and a time step of 2.0 femtosecond (fs). Molecular dynamics were performed at 300 K using a residue-based cut-off of 10 Å. Pairlists were updated every 25 time steps. Hydrogens were added to the structure predicted by MODELLER using the stored internal coordinates of the AMBER all-atom data base and then minimized, the heavy atoms being kept fixed in their original positions. All Lys and Arg residues were positively charged and Glu and Asp residues were negatively charged.

The reduced form of the cofactor (NADPH) was used for the calculations, according to the tighter binding of NADPH over NADP^+ to DHFR.^{31–33} Force field parameters for NADPH were adapted from previous simulations that employed the oxidized form (NADP^+) of the cofactor.³⁴ The geometry of the reduced nicotinamide ring was fully optimized at the 6-31G* level using Gaussian 94, and partial charges on atoms were calculated from an electrostatic potential fit to a 6-31G* ab-initio wave function, followed by a standard RESP (restrained electrostatic potential) fit.^{35,36} Bond, angle, dihedral and van der Waals parameters of the nicotinamide ring were assigned consistently with the Cornell et al. force field, and then tested for their ability to reproduce the 6-31G* optimized geometry. The remaining adenosine and phosphate parameters of NADPH were taken from NADP^+ .³⁴

Molecular mechanics and molecular dynamics calculations on the two long insertions in the pfDHFR sequence were performed first to allow more relaxation of the non-conserved and less validated regions of the structure without affecting the geometry of the most conserved regions. The two loops were energy-minimized with 3000 steps of conjugate gradient minimization, followed by 10 ps molecular dynamics at 300 K. This protocol was repeated 10 times, with energy-minimization after each molecular dynamics. To perform these first molecular mechanics and molecular dynamics calculations, a distance-dependent dielectric constant with a dielectric multiplication constant of 4 was used to simulate the presence of water.

In order to include the effects of explicit water molecules at the active site of DHFR, the final structure obtained was solvated with a spherical cap of 2113 TIP3P³⁷ water molecules centered on the center of mass of pfDHFR. Calculations were continued using a dielectric constant of 1 and the explicit water molecules. In order to allow the equilibration of the solvent around the protein residues, 100 ps molecular dynamics at 300 K were performed on the water molecules. Then, the whole system (enzyme, water, and NADPH) was energy-minimized with 3000 steps, with 5 Kcal/mol restraint applied on the backbone atoms of the enzyme with the exception that the backbone atoms of loops 1 and 2 were left free. The restraint was imposed in order to avoid initial large drifts from the homology model structure, which is based on experimentally-validated structures of DHFRs. Then, 2000 steps of minimization without any constraints were performed, and the resulting structure was compared with the homology model and the DHFR templates to ensure that the conserved regions maintained similar 3D-structure. A 200 ps molecular dynamics simulation at 300 K was then performed on the whole system with a 1 Kcal/mol restraint on the backbone atoms. Whilst performing molecular dynamics, coordinates were collected every 0.2 ps and averaged every 10 ps for visual inspection. Finally, 2000 steps of energy-minimization without constraints were performed. The values of RMS deviations between the final pfDHFR model and the crystal structures of DHFRs from different sources used for homology modeling

were calculated. The considerably low RMS deviations, 1.40 with *E. coli*, 1.47 with *L. casei*, 1.21 with human, 1.24 with chicken liver, and 1.26 with *P. carinii*, revealed that the pfDHFR model was close to these structures.

Docking of pyrimethamine, cycloguanil and WR99210, and molecular dynamics of the complexes

The inhibitors were docked into the active site of pfDHFR, using the final structure obtained from the explicit solvent molecular dynamics calculations. The inhibitors were modeled as protonated state at N1, as evidenced by the NMR studies of both the bound and free states of Pyr, methotrexate (MTX) and trimethoprim (TMP).^{38,39} The protonated amino portions of the inhibitors were initially positioned to interact with the anionic side chain of D54. This choice was strongly suggested by the binding modes of other antifolates with the conserved aspartic or glutamic acid residue corresponding to D54 of the pfDHFR in the available crystal structures of DHFRs from different sources. While Pyr and Cyc have conformationally constrained structures, the more conformationally flexible 2',4',5'-trichlorophenoxy propyloxy group of WR99210 was docked into the active site using the orientations of folate and MTX in the available crystal structures as guidelines.

To obtain a set of atomic charges for the inhibitors, their structures were completely optimized at the STO-3G basis set level, using Gaussian 94. Charges were calculated from an electrostatic potential fit to a 6-31G* ab-initio wave function, followed by a standard RESP fit. Atom types were assigned consistently with the Cornell et al. force field,²⁹ and some parameters were adjusted to reproduce the STO-3G optimized geometry. The parameters for the chlorine atoms of the inhibitors were as previously described.⁴⁰

The molecular mechanics and molecular dynamics calculations of the complexes with the inhibitors were performed in explicit water molecule environment. The same solvation sphere of the pfDHFR–NADPH binary complex was used, but the water molecules that are replaced by the inhibitors were removed from the structure. Two thousand steps of minimization on the inhibitor, NADPH, the water molecules and all the protein residues within 10 Å from the inhibitor were performed, followed by 300 ps molecular dynamics at 300 K. A 1 Kcal/mol restraint on the backbone atoms was applied to avoid undesirable drifts from the initial structure.

Molecular dynamics of the pfDHFR mutant complexes

The mutant pfDHFRs complexed with Pyr, Cyc and WR99210 were constructed by changing alanine to valine (A16V), serine to threonine (S108T), and both (A16V + S108T) in the corresponding structures of the wild-type pfDHFR–inhibitor complexes. Five hundred steps of energy-minimization were performed on the inhibitor and the mutated residue only in order to position the side chain of valine and/or threonine with respect to the inhibitor and to relieve steric conflicts due

to the growing of the bulkier amino acid side chains. This was followed by 1000 steps of minimization on the protein residues within 10 Å from the inhibitor, the inhibitor, and all the water molecules. The molecular dynamics at 300 K was then started from these minimized complexes and run for over 300 ps. The 1 Kcal/mol restraint on the backbone atoms was applied as usual.

Synthesis of derivatives of cycloguanil and WR99210

Compounds **I**, **II**, **III**, **XIV** and **XV** were prepared by a three-component condensation between 4-chloroaniline, dicyanodiamide and acetone in the presence of concentrated HCl (**I**) or two-component condensation between the arylbiguanides and the aldehydes (**II**, **III**, **XIV** and **XV**) both in the presence of concentrated HCl according to the literature.^{41–45} The new compound **IV** was synthesized by a three-component condensation between 4-chloroaniline, dicyanodiamide and methylal. Compounds **V–XII** were synthesized by a modified two-component condensation⁴⁴ between the corresponding biguanides and ketones in the presence of concentrated HCl as catalyst and triethyl orthoacetate as water scavenger, the details of which will be published elsewhere (Vilaivan et al., in preparation). All cycloguanil derivatives were isolated as monohydrochloride salts and were purified by crystallization from water or water–ethanol. New compounds gave clean ¹H nmr and mass spectra (APCI or MALDI) and provide satisfactory elemental analysis (C,H,N).

Preparation of pfDHFRs and inhibitor binding studies

The recombinant plasmids pET-pfDHFR (wild-type) and pET-pfDHFR (A16V+S108T) were prepared as previously described¹⁰ and were employed for the preparation of enzymes used for testing the compounds synthesized in the present study. Purification of both wild-type and mutant pfDHFRs was achieved by affinity chromatography on MTX-Sepharose CL-6B column.⁴⁶ The activity of pfDHFR was determined spectrophotometrically by monitoring the decrease in absorbance at 340 nm at 25 °C according to the standard assay method described previously.⁴⁶ For determination of the *K_i* values of a number of synthesized analogues, the assay reactions were initiated with affinity-purified enzyme (~0.005–0.01 U ml⁻¹), and the initial velocities in the presence of varying concentrations of inhibitors were analyzed by non-linear least square fit using KaleidagraphTM software. Other analyses of the protein were as earlier described.¹⁰

Results

The alignment of the sequence of pfDHFR with the sequences of DHFRs from selected sources of which the X-ray structures are known is shown in Figure 1. There is significant homology among the DHFRs compared, with the exception that the pfDHFR sequence contained two extra insertions between residues 22–38 and residues 64–98. Our initial pfDHFR model was therefore

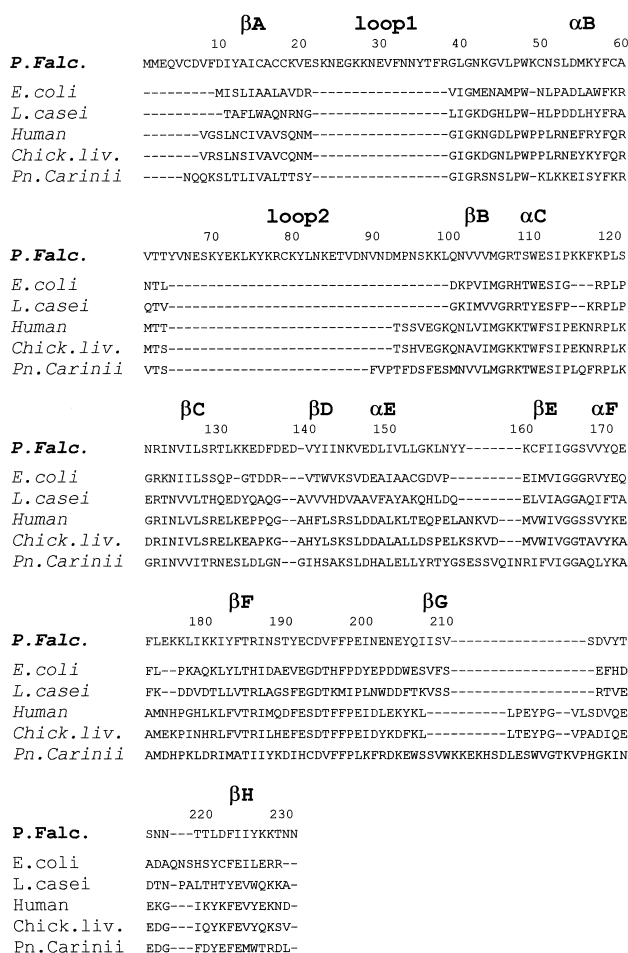


Figure 1. Alignment of the amino acid sequences of dihydrofolate reductase of *Plasmodium falciparum*,¹⁸ *Escherichia coli*,⁴⁹ *Lactobacillus casei*,⁵⁰ human,^{51,52} chicken liver,⁵³ and *Pneumocystis carinii*.⁵⁴ The percentages of the identical amino acids between *P. falciparum* DHFRs and DHFRs from *E. coli*, *L. casei*, human, chicken liver, and *P. carinii* are 29, 24, 32, 32, and 24%, respectively. The elements of secondary structure are indicated as α , β , and loop.

constructed without the sequences of the two insertions. The resulting model was then used to check for the folding of the conserved regions, to make superimpositions and comparisons with other known templates.

The local alignments of the two extra sequences of pfDHFR were predicted from BLAST.²⁶ A stringent significance threshold of 3 was adopted, resulting in two significant homologous segments for loop 1 and five for loop 2. The predicted alignments were restored into the DHFR model. As for loop 1, the local alignments predicted to fill this insertion significantly reduced the quality of the model and also markedly affected the structure of the most conserved regions. On the contrary, one out of the five local alignments that BLAST identified to fill the second insertion gave an acceptable initial arrangement of loop 2 without affecting the quality and the structure of the conserved regions. Therefore, the initial homology model was constructed using the best local alignment only for loop 2. The loop 1, however, was subsequently constructed manually and then appended to the structure previously obtained

from MODELLER, with some adjustment. It is important that the homology model be maintained as close as possible to the experimentally-validated DHFRs in the conserved regions, though only an initial guess of the conformation could be obtained at this stage for the two loops. Extensive molecular dynamics calculations were performed in order to obtain the best conformation, first on the two loops and subsequently on the whole pfDHFR structure. A restraint on the backbone atoms of the conserved regions of DHFR during molecular dynamics prevented undesirable drifts from the crystal structures of the templates. The final model obtained is graphically displayed in Figure 2.

The overall folding of pfDHFR is very similar to that previously reported for other DHFRs.⁴⁷ An eight-stranded β -sheet (β A– β H) consisting of seven parallel strands and a carboxyl terminal antiparallel strand composes the core of the protein. Four α helices (α B, α C, α E, α F) are packed against the β sheet core. The two-turn character of helix α E, which is present in the human and chicken liver DHFRs but not in the *E. coli* and *L. casei* DHFRs, is not predicted in the pfDHFR structure. The remaining residues are involved in loops, which connect elements of secondary structure.

NADPH is bound to pfDHFR in an extended conformation similar to that previously reported for co-factor binding to other DHFRs, with nearly all the protein–cofactor interactions being conserved within available crystal structures (data not shown). The nicotinamide ring is bound near the center of the molecule in a cleft formed by the divergence of β E and β A. The A-side of nicotinamide is directed towards the opening of the active site. The 3'-carboxamide amino group hydrogen bonds to the backbone oxygen of A16, and the

carboxamide carbonyl hydrogen bonds to the backbone nitrogen of A16.

Docking of Pyr, Cyc, and WR99210 into the active site of the pfDHFR models was performed to investigate the interactions of the drugs with various amino acid residues in the active site of both wild-type and A16V+S108T mutant DHFR models. The selected active site residues of the wild-type pfDHFR model that interacted with Cyc (shown as green) is illustrated in Figure 3A; the 6-amino group of Cyc hydrogen bonds to one carboxylate oxygen of D54, which in turn forms hydrogen bond to T185, and the protonated N1–H of Cyc hydrogen bonds to the other carboxylate oxygen of D54. The bidentate hydrogen bonding observed with the residue D54 is not uncommon and indeed is consistent with the specific hydrogen bonding interactions established between the amino functions of antifolates and the conserved aspartic or glutamic acid side chains of other DHFRs whose crystal structures are available. The 4-amino group of Cyc hydrogen bonds to the backbone oxygens of I164 and I14, while the 2,2'-dimethyl groups are in contact with A16, L46, and F58 side chains. Finally, the 3-chlorophenyl substituent of Cyc stacks against the nicotinamide ring of NADPH, with the chlorine atom close to S108 and I112. The binding of Pyr and WR99210 to the wild-type DHFR was found to be very similar to Cyc (Fig. 3, Panel A), whereas this is not the case for the A16V+S108T mutant pfDHFR (Fig. 3, Panel B). The differences in the orientation and binding interactions of the inhibitors were better highlighted from the superimpositions of the inhibitors in the active site of the wild-type pfDHFR model. As shown in Figure 4, the three inhibitors, i.e., Pyr (yellow), Cyc (green) and WR99210 (red), were very well superimposed and showed nearly identical interactions

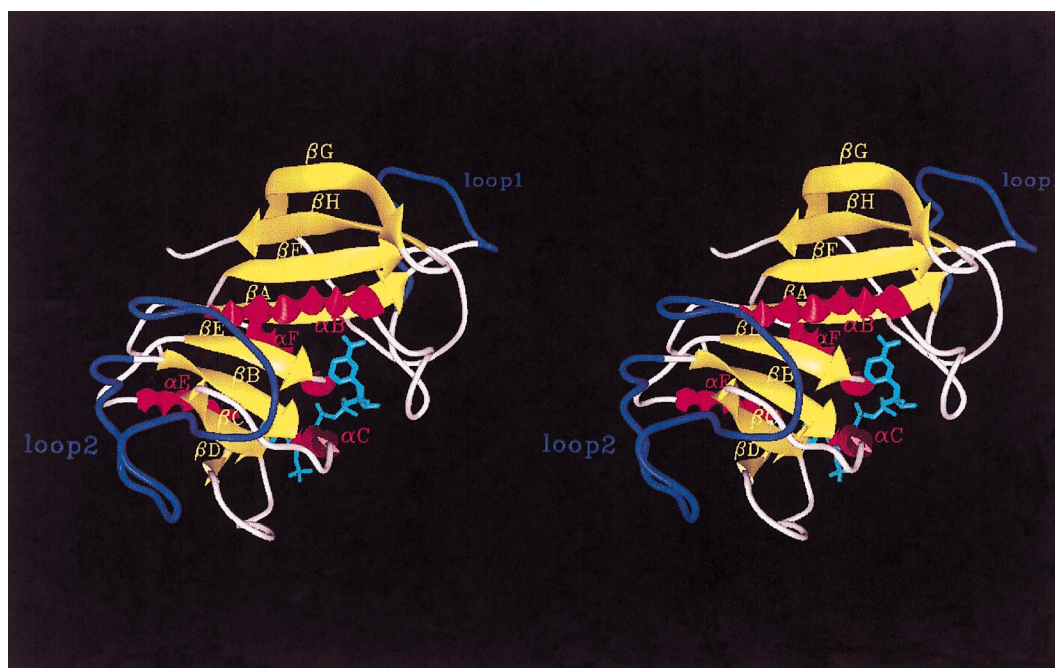


Figure 2. Stereoviews showing the overall folding of *Plasmodium falciparum* DHFR. β sheets are colored in yellow, α helices are colored in red. The loops are white, with the exception of loops 1 and 2 corresponding to the two insertions in pfDHFR which are colored in blue. NADPH is colored in cyan.

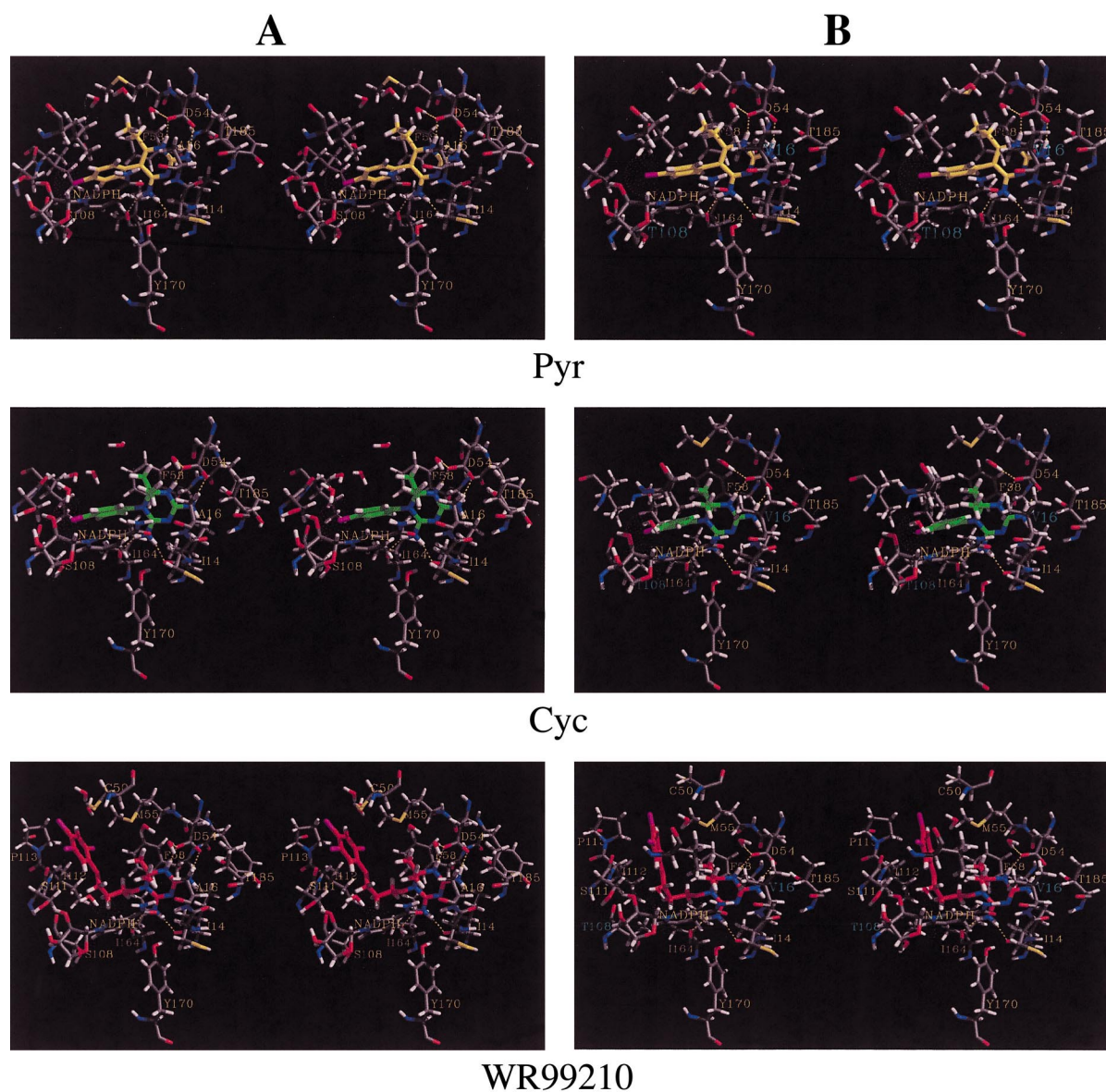


Figure 3. Stereoviews of wild-type (Panel A) and A16V + S108T (Panel B) pfDHFRs showing active site residues involved in the interaction with Pyr (yellow), Cyc (green), and WR99210 (red). The residues shown are I14, A16, C50, D54, M55, F58, S108, S111, I112, P113, I164, Y170 and NADPH molecule.

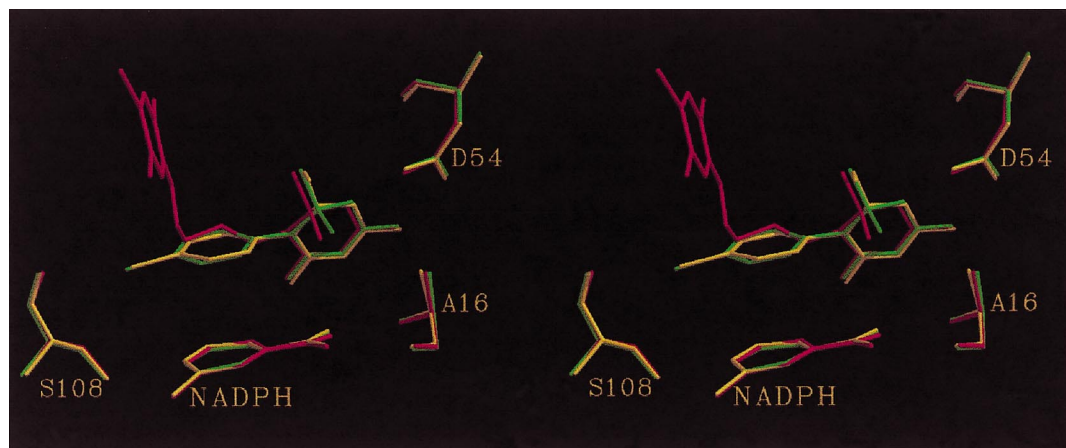


Figure 4. Stereoviews showing the superimpositions of inhibitors bound at the active site of wild-type pfDHFR. Residues A16, D54, S108, and the nicotinamide ring of NADPH are shown with the inhibitors Pyr (yellow), Cyc (green), and WR99210 (red).

with the same residues as those described for Cyc. However, while the chlorophenyl substituent of Cyc and Pyr stacks against the nicotinamide ring of NADPH and is directed toward S108, the flexible trichlorophenoxy propyloxy of WR99210 is almost perpendicular with the nicotinamide ring and is not in contact with the cofactor. Interestingly, one water molecule binds over the nicotinamide ring, making hydrogen bonds with the N1 nitrogen of the nicotinamide and the 2'-hydroxyl of the ribose. The trichlorophenoxy propyloxy substituent of WR99210 is in contact with C50, M55, S111, and P113 (see Fig. 3A and B).

The effects of single and double mutations at amino acid residues 16 and 108 on the binding of Pyr, Cyc and WR99210 were further investigated (Fig. 5). The molecular dynamics stimulation of the Pyr complexed with A16V mutant model revealed minimal changes of orientation and binding interactions with respect to that of the wild-type enzyme complex (Fig. 5A). By contrast, the complex between Cyc and the A16V mutant was significantly different from the complex with the wild-type enzyme; the inhibitor was displaced from its position in the wild-type complex due to the steric conflict with valine in A16V mutant (Fig. 5B). Superimposition between Cyc and Pyr in the wild-type complexes indicated that one of the two 2,2'-methyl substituents of Cyc was located much closer (1.4 Å) to the methyl of the A16 side chain with respect to the 6-ethyl substituent of Pyr, the former being in Van der Waals contact with the methyl of A16 whereas the latter is significantly more distant (data not shown). Therefore, the steric demand imposed by the A16V mutation should be much more pronounced for Cyc than for Pyr, although hydrogen bonding interactions with D54, I14, and I164 are still present. The displacement of Cyc in the structure of the A16V mutant is illustrated in Figure 5B. While the displacement of the triazine ring of Cyc did not seem to affect the ability to make hydrogen bond between the drug and D54, I14, and I164, the orientation of the chlorophenyl ring of the inhibitor bound to the A16V enzyme was found to be significantly different from that of the wild-type enzyme. This is due to Cyc being bound in a locked region comprising A16 and D54 for the dihydrotriazine ring, nicotinamide, and S108 for the chlorophenyl ring of the inhibitor. Interestingly, the stacking interactions with the nicotinamide ring of NADPH were completely lost in the A16V mutant and one water molecule was found in place of the chlorophenyl ring (data not shown).

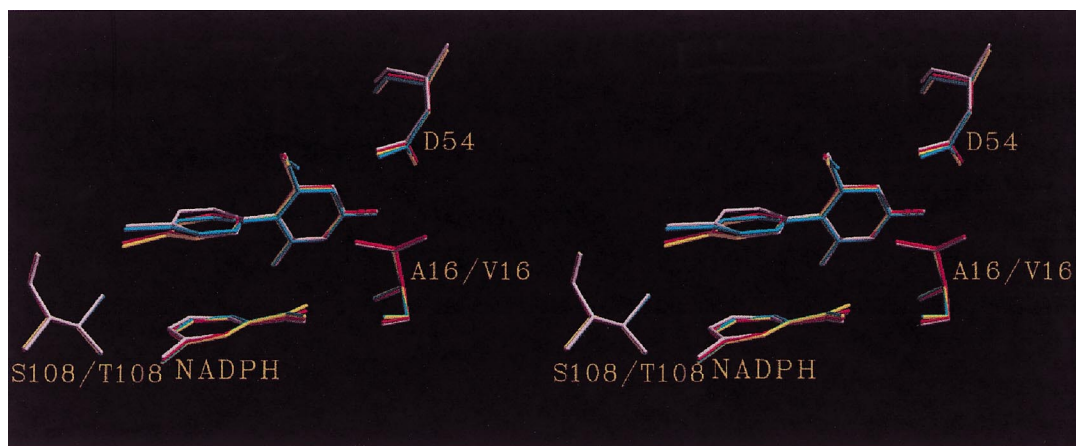
The dihydrotriazine rings of WR99210 and Cyc are identical and therefore are predicted to bind the A16V mutant pDHFR in the same orientation. As a consequence, the 2,2'-dimethyl substituents of WR99210 should also be in steric conflict with the valine side chain of the A16V mutant. Figure 5C illustrates the superimpositions of WR99210 bound to wild-type, A16V, S108T and A16V+S108T double mutant DHFR models. A slight displacement from its optimal position occupied in the wild-type complex was noted when the inhibitor was bound to the pDHFRs with A16V mutation. The model shows that the trichlorophenoxy

propyloxy substituent of WR99210 is not forced to change its orientation significantly in the A16V mutant. Instead, its flexible side chain allows it to be free from being locked between the residues A16, D54, nicotinamide, and S108 as observed in the structure of the wild-type complex. Therefore it is likely that the steric demand imposed by V16 would not significantly affect the orientation of the drug upon binding to the pDHFRs with the A16V mutation (Fig. 5C).

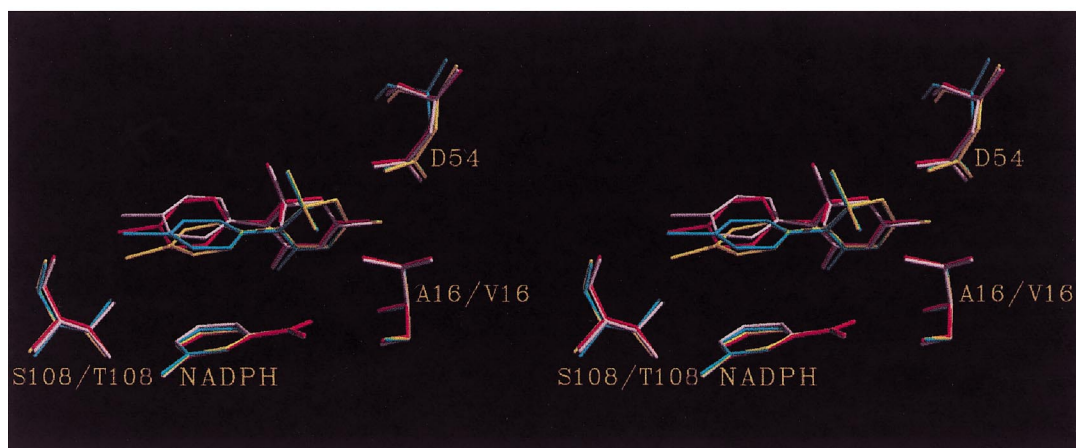
The bindings of Pyr, Cyc, and WR99210 to the mutant model of DHFR with single S108T mutation were also investigated. Generally, all the three inhibitors bind to the S108T mutant model with similar orientation as in the wild-type complex, albeit with some minor differences. The bulkier side chain of the T108 mutant slightly affects the position of the chlorophenyl ring of Pyr and Cyc (Fig. 5A and B). However, the orientation of the propyloxy substituent of WR99210 is not affected upon binding to pDHFR with the S108T mutation (Fig. 5C).

The model indicates that the 6-ethyl substituent of Pyr is not in steric conflict with A16V+S108T pDHFR despite the locking of the inhibitor between residues 16, 54, nicotinamide, and 108. Therefore, Pyr is predicted to bind the double mutant DHFR with no appreciable differences as compared to the binding to the wild-type, A16V, and S108T single mutant enzymes (Fig. 5A). As previously illustrated for the A16V and S108T mutant, the steric conflict with V16 must be relatively small and therefore no significant displacement of the inhibitors was detected. The situation is very different for Cyc. In the A16V+S108T double mutant, however, the chlorophenyl ring is further displaced from nicotinamide owing to steric conflicts with T108, while the position of the dihydrotriazine ring of Cyc is not different to that of the A16V mutant (Fig. 5B). Binding of WR99210 is similar to Cyc in its dihydrotriazine moiety but the inhibitor is not locked toward nicotinamide and is also much more flexible. As a result, slight displacement of the dihydrotriazine ring has no consequences for the overall binding in the double mutant enzyme (Fig. 5C). The steric clash between the V16 side chain of the A16V mutant pDHFR is clearly evidenced for Cyc binding, but not for Pyr binding (Fig. 6).

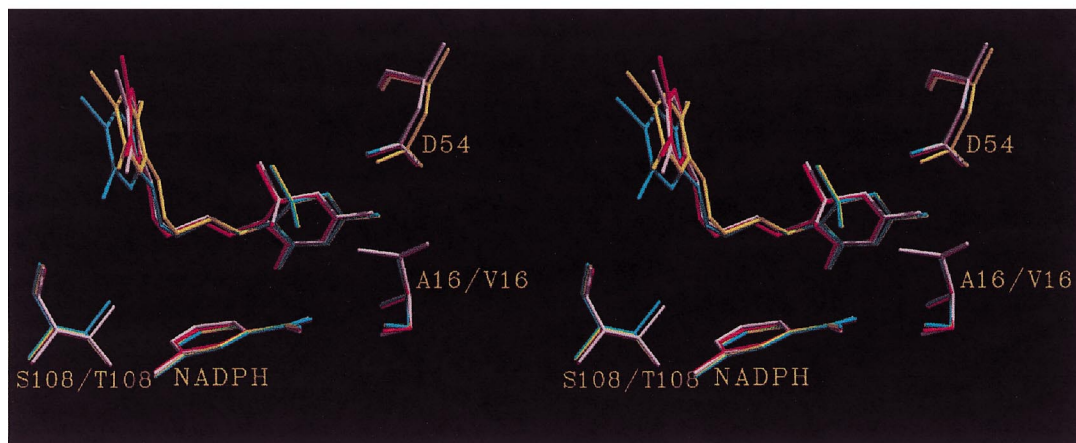
In order to verify the homology model of *P. falciparum* DHFR and to exploit the model for the prediction of binding of inhibitors and/or development of strategies for the design of the best effective inhibitor(s) targeted against antifolate resistant malaria, we have synthesized a number of Cyc derivatives and tested against both wild-type and A16V+S108T mutant pDHFRs. Our premise is that resistance to Cyc in the A16V+S108T mutant is the result of steric conflict imposed by a bulkier side chain of V16. To test the hypothesis, Cyc derivatives with one substituent (ethyl or methyl group) or no substituent at position R₂, and those with bulky substituents at both R₁ and R₂ positions of the dihydrotriazine ring were synthesized. The binding affinity (*K_i*) values were then determined and the ratios of *K_i*-mut/*K_i*-wt were compared. Table 1 summarizes the *K_i*



(A)



(B)



(C)

Figure 5. Superimpositions of inhibitors bound to wild-type (yellow), A16V (red), S108T (cyan) and A16V+S108T (white) pDHFRs. The inhibitors shown are (A) Pyr; (B) Cyc; (C) WR99210.

values for the wild-type and the A16V+S108T mutant DHFRs. The relative loss in binding affinity of the Cyc derivatives is reflected by the elevation of $K_i\text{-mut}/K_i\text{-wt}$ ratio. As shown in Table 1, the compounds **II** and **III** inhibited the wild-type pDHFR with K_i values 2–3 times higher than that of Cyc, but exhibited 7–10 times lower K_i values for the A16V+S108T mutant pDHFR

than the Cyc. As a result, the $K_i\text{-mut}/K_i\text{-wt}$ ratios for the compound **II** and **III** were ~17–28 times lower than that of the Cyc parent compound. Removal of both methyl groups at the 2- R_1 and 2- R_2 positions gave rise to compound **IV** (didesmethyl Cyc), which has a K_i value for the wild-type enzyme about 16-fold higher than that of Cyc, whereas the K_i value for the A16V+S108T enzyme

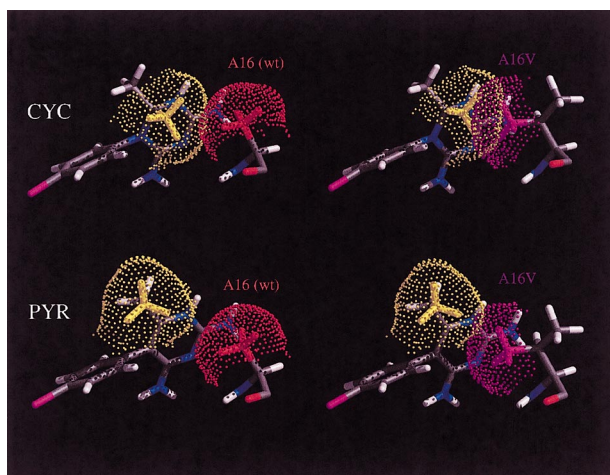


Figure 6. Display of the surface of the side chain residue of amino acid A16 (red) and A16V (purple) interacting with one of the 2,2'-methyl substituents of Cyc (yellow) and 6-ethyl substituent of Pyr (yellow).

was about 2-fold lower than Cyc. As a consequence, the ratio of $K_i\text{-mut}/K_i\text{-wt}$ for the compound **IV** was 34-fold lower than that for Cyc (Table 1).

Our studies were further extended to investigate the binding between Cyc derivatives with bulky 2,2' di-substituents and the wild-type and A16V + S108T mutant DHFRs. Nine compounds (compounds **V–XIII**) were selected for the evaluation. Except for compounds **IX** and **XIII**, which exhibited high K_i values, all other seven derivatives gave K_i values for the wild-type enzyme that were comparable to that for Cyc. When tested with the A16V + S108T enzyme, the K_i values of these derivatives except compound **VIII** were all higher than that of Cyc, resulting in relatively high ratios of $K_i\text{-mut}/K_i\text{-wt}$.

The K_i values for WR99210 (compound **XIV**, Table 2) and other Cyc derivatives were compared with their 2-monomethyl derivatives (Table 2). Removal of one methyl from position 2- R_1 of WR99210 (compound

XV, Table 2) resulted in a 2- and 3-fold decrease in the K_i values for the wild-type and the A16V + S108T enzymes, respectively. The compound **XVI** with 4'-Br- C_6H_4 at 3-R position (Table 2) only slightly increased the K_i for the wild-type pfDHFR by 2-fold, but dramatically elevated the K_i for the A16V + S108T enzyme by 800-fold. The steric conflict observed in the compound **XVI** was relieved by replacing the methyl group at position 2- R_1 with hydrogen. The resulting compound **XVII** was then found to exhibit a 10-fold lower K_i for the A16V + S108T enzyme as compared to the compound **XVI**, albeit the manipulation slightly affected the binding affinity of the inhibitor to the wild-type enzyme. Likewise, similar effect was also found for compounds **XVIII** and **XIX**, where changes were made at the positions 2- R_1 and 3-R (Table 2).

Discussion

Resistance to antifolates Pyr and Cyc in malaria parasites has been shown to be associated with point mutations in the *dhfr* gene.^{1,5,7,46} Cross resistance to both drugs is generally found to involve combinations of N51I, C59R, S108N, and I164L mutations, whereas parasites resistant to Cyc but susceptible to Pyr are associated with mutation at residues 16 and 108 (A16V + S108T). In the present study, we sought to understand the molecular interactions between the DHFR of *P. falciparum* and antimalarial antifolates Pyr, Cyc, and WR99210, to predict the effect of mutation(s) on the binding of the inhibitors to the enzyme, and to address the importance of the mutation(s) at different residues in conferring resistance to the antifolates.

We describe a homology model of *P. falciparum* DHFR based on sequence alignment of the DHFR sequences of *E. coli*, *L. casei*, human, chicken liver, and *P. carinii*. Our model was built using the conserved regions of a number of known DHFR templates, and the structures of the unique regions in pfDHFR were subsequently assigned to avoid undesirable perturbation of

Table 1. K_i values for the cycloguanil derivatives with only one or no substituent at position R_1 (compounds **I–IV**) and bulky substituents at positions R_1 and R_2 (compounds **V–XIII**)^a

Compound	2- R_1	2- R_2	$K_i\text{-wt}^b$ (nM)	Rel to Cyc	$K_i\text{-mut}^c$ (nM)	Rel to Cyc	$K_i\text{-mut}^c/K_i\text{-wt}^b$
I	Me	Me	1.5 ± 0.3^d	1.0	1314 ± 165^d	1.0	876
II	H	Me	4.1 ± 0.0	2.7	127 ± 14	0.1	31
III	H	Et	3.6 ± 0.0	2.4	189 ± 37	0.14	53
IV	H	H	24.4 ± 4.3	16.3	646 ± 78	0.5	26
V	Me	<i>n</i> -Pr	3.5 ± 0.4	2.3	9229 ± 547	7.0	2637
VI	Me	<i>n</i> -Bu	1.8 ± 0.2	1.2	4217 ± 390	3.2	2343
VII	Me	<i>n</i> -Pen	1.2 ± 0.1	0.8	3594 ± 446	2.7	2995
VIII	Me	<i>n</i> -Hex	0.6 ± 0.1	0.4	956 ± 78	0.7	1593
IX	Me	<i>i</i> -Pr	36.5 ± 4.1	24.3	$44,791 \pm 5872$	34.1	1227
X	Me	<i>i</i> -Bu	4.7 ± 1.9	3.1	$15,263 \pm 986$	11.6	3247
XI	Me	<i>i</i> -Pen	1.7 ± 0.1	1.1	5755 ± 545	4.4	3385
XII	Et	Et	7.7 ± 1.2	5.1	$16,151 \pm 3599$	12.3	2098
XIII	Et	<i>n</i> -Pen	19.3 ± 3.8	12.9	$18,041 \pm 1905$	13.7	935

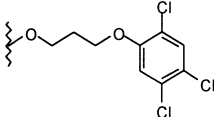
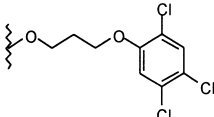
^aMe, methyl; Et, ethyl; Pr, propyl; Bu, butyl; Pen, pentyl; Hex, hexyl.

^bWild-type pfDHFR.

^cpfDHFR (A16V + S108T).

^dData from Sirawaraporn et al.¹⁰

Table 2. K_i values for the WR99210 and other cycloguanil derivatives compared with their 2-monomethyl derivatives

Compound	3-R	2-R ₁	2-R ₂	K_i -wt ^a (nM)	Rel to WR99210	K_i -mut ^b (nM)	Rel to WR99210	K_i -mut ^b / K_i -wt ^a
XIV (WR99210)		Me ^c	Me	0.5 ± 0.1	1.0	2.4 ± 0.4	1.0	4.8
XV		H	Me	0.3 ± 0.0	0.6	0.8 ± 0.1	0.3	2.7
XVI	4'-Br-C ₆ H ₄	Me	Me	1.1 ± 0.2	2.2	1948 ± 366	812	1771
XVII	4'-Br-C ₆ H ₄	H	Me	5.7 ± 0.5	11.4	202 ± 17	84	35
XVIII	4'-Me-C ₆ H ₄	Me	Me	1.8 ± 0.2	3.6	1584 ± 210	660	880
XIX	4'-Me-C ₆ H ₄	H	Me	23.4 ± 1.9	46.8	186 ± 22	78	8.0

^aWild-type pfDHFR.^bpfDHFR (A16V + S108T).^cMe, methyl.

the overall conformation of the structure. The overall topology of the pfDHFR is similar to the DHFRs from other sources (Fig. 2), except for its two extra-loop insertions located at the enzyme surface. Unlike those previously reported by other workers,^{18,48} the model presented in this paper was built based not only on the alignments among the DHFR sequences, but also on their 3D-structural conservation. The homology noted at least from residue 10, therefore, makes the alignment more meaningful and enables analysis of residue 16 which is crucial for Cyc-resistance. In the present study, the structures of A16V and A16V + S108T mutant pfDHFRs were also built from the wild-type template and docking of the antifolates Pyr, Cyc, and WR99210 was performed using both wild-type and mutant structures.

Our structural models show that the ethyl and methyl substituents of Pyr and Cyc, respectively, are directed towards the methyl side chain of A16 in the wild-type pfDHFR. As a result, it is very likely that the bulkier side chain of valine in the A16V mutant of pfDHFR would cause steric conflicts with these substituents, and therefore may explain Cyc resistance for these mutants. However, such effect does not occur in the case of Pyr; the inhibitor binds equally well with the same orientation and binding interactions to A16V + S108T mutant pfDHFR as well as the wild-type enzyme, evidence which is in accord with the earlier observations by many groups that the A16V + S108T mutant is susceptible to Pyr.^{5,7,10,11}

Although Cyc is predicted to bind to the wild-type pfDHFR in a similar way to Pyr, one of its two 2,2'-dimethyl substituents is significantly closer to the side chain of residue 16 than is the ethyl group of Pyr. This would inevitably generate steric constraint for binding to Cyc when the bulkier side chain of valine is present at position 16 as in the A16V and A16V + S108T mutants. Since Cyc is predicted to bind in a locked region which is composed of A16 and D54 for the dihydrotriazine

ring, and nicotinamide and S108 for the chlorophenyl ring of the inhibitor, A16V + S108T mutation would result in steric constraint and cause displacement of both the dihydrotriazine moiety and the chlorophenyl ring from its optimal position as depicted for the wild-type enzyme, giving rise to a remarkable loss of binding affinity for Cyc and hence resistance to Cyc for the A16V + S108T mutant pfDHFR.

The displacement of WR99210, however, is relatively minor when compared with Cyc. This is likely due to the reason that the more flexible trichlorophenyl propoxy side chain of WR99210 is not locked between nicotinamide and S108 as observed for the chlorophenyl ring of Cyc. Therefore, the steric demand imposed by valine 16 only slightly affects the orientation of WR99210 and leaves unaffected binding interactions with other protein residues, in agreement with the finding that WR99210 is highly effective against the resistant mutants.

Our model predicts that binding of the derivatives with only one or no substituent at position 2 should be less affected by the mutation than Cyc. This would be reflected in the values of the ratios of the K_i for the A16V + S108T mutant enzyme and the wild-type enzyme (K_i -mut/ K_i -wt). In order to test this model, a number of Cyc derivatives were synthesized and the binding affinities to the wild-type and mutant enzymes were studied. It was found that K_i -mut/ K_i -wt values for the derivatives with only one or no substituent at position 2 are lower than for Cyc, as predicted (compounds **II–IV**, Table 1). Furthermore, 2,2'-disubstituted derivatives of Cyc with bulky substituents tend to have higher K_i -mut/ K_i -wt ratios, as expected (compounds **V–XIII**, Table 1). The favorable effect on binding of the removal of the 2-methyl group was also found for WR99210 (Table 2). However, this effect is far less than for Cyc derivatives with p-chloro-, bromo- or methyl-phenyl substituents, because WR99210 is not locked, and can already interact well with the mutant enzyme even with

both 2-methyl groups present. The overall results obtained from this study are in support of the steric constraint hypothesis. Further it reveals the important steric role in binding between the substituents at position 2 of Cyc to the active residue(s) of the pfDHFR, which could have profound implications for the development of new and effective inhibitors against antifolate resistant parasites.

Conclusion

The homology models of wild-type, A16V, S108T, and A16V+S108T *P. falciparum* DHFRs were built based on multiple sequence alignment and homology modeling procedures. The models were used to address the molecular interactions between the active site residues of the enzymes and antifolates Cyc, Pyr and WR99210. We proposed a 'steric constraint' hypothesis and demonstrated its validity by testing with inhibitor analogues using the wild-type and relevant mutant pfDHFRs. The models not only explain the Cyc resistance but also Pyr susceptibility in relation to the A16V mutation of the pfDHFR domain. In addition, it has allowed us for the first time to better understand the molecular basis of cross resistance between Cyc and Pyr, which have been known to involve mutations at residues 51, 59, 108 and 164 of the pfDHFR domain. Further, the modeling of the interaction between pfDHFR and WR99210 has also provided ideas that could lead to the development of new and more effective second generation antifolate antimalarials.

Acknowledgements

This research is supported by grants from World Health Organization (TDR) to WS, the European Union (INCO-DC IC18CT970223) to YY and GL, and The University of Modena (Ricerca Orientata) to GR. TV is supported by The Thailand Research Fund (PDF/57/2540). We thank Rachada Sirawaraporn and Kaneung Chitcholtan for their excellent technical assistance.

References

- Cowman, A. F.; Morry, M. J.; Biggs, B. A.; Cross, G. A. M.; Foote, S. J. *Proc. Natl. Acad. Sci. USA* **1988**, *85*, 9109.
- Snewin, V. A.; England, S. M.; Sims, P. F. G.; Hyde, J. E. *Gene* **1989**, *76*, 41.
- Basco, L. K.; de Pecoulas, P. E.; Le Bras, J.; Wilson, C. M. *Exp. Parasitol.* **1996**, *82*, 97.
- Basco, L. K.; de Pecoulas, P. E.; Wilson, C. M.; Le Bras, J.; Mazabraud, A. *Mol. Biochem. Parasitol.* **1995**, *69*, 135.
- Foote, S. J.; Galatis, D.; Cowman, A. F. *Proc. Natl. Acad. Sci. USA* **1990**, *87*, 3014.
- Hyde, J. *Parasitol. Today* **1989**, *5*, 252.
- Peterson, D. S.; Walliker, D.; Welles, T. E. *Proc. Natl. Acad. Sci. USA* **1988**, *85*, 9114.
- Thaithong, S.; Chan, S.-W.; Songsomboon, S.; Wilairat, P.; Seesod, N.; Sueblinwong, T.; Goman, M.; Ridley, R.; Beale, G. *Mol. Biochem. Parasitol.* **1992**, *52*, 149.
- Zolg, J. W.; Plitt, J. R.; Chen, G.-X.; Palmer, S. *Mol. Biochem. Parasitol.* **1989**, *36*, 253.
- Sirawaraporn, W.; Sathitkul, T.; Sirawaraporn, R.; Yuthavong, Y.; Santi, D. *Proc. Natl. Acad. Sci. USA* **1997**, *94*, 1124.
- Peterson, D. S.; Milhous, W. K.; Welles, T. E. *Proc. Natl. Acad. Sci. USA* **1990**, *87*, 3018.
- Childs, G. E.; Lambros, C. *Ann. Trop. Med. Parasitol.* **1986**, *80*, 177.
- Hekmat-Nejad, M.; Rathod, P. K. *Exp. Parasitol.* **1997**, *87*, 222.
- Sanchez, R.; Sali, A. *Curr. Opin. Struct. Biol.* **1997**, *7*, 206.
- Toyoda, T.; Brobey, R. K. B.; Sano, G.-I.; Horii, T. *Biochem. Biophys. Res. Commun.* **1997**, *235*, 515.
- McKie, J. H.; Douglas, K. T.; Chan, C.; Roser, S. A.; Yates, R.; Read, M.; Hyde, J. E.; Dascombe, M. J.; Yuthavong, Y.; Sirawaraporn, W. *J. Med. Chem.* **1998**, *41*, 1367.
- Warhurst, D. C. *Drug Discovery Today* **1998**, *3*, 538.
- Bzik, D. J.; Li, W.-B.; Horii, T.; Inselburg, J. *Proc. Natl. Acad. Sci. USA* **1987**, *84*, 8360.
- Reyes, V. M.; Sawaya, M. T.; Brown, K. A.; Kraut, J. *Biochemistry* **1995**, *34*, 2710.
- Bolin, J. T.; Filman, D. J.; Matthews, D. A.; Hamlin, R. C.; Kraut, J. *J. Biol. Chem.* **1982**, *257*, 13650.
- Oefner, C.; D'Arcy, A.; Winkler, F. K. *Eur. J. Biochem.* **1988**, *174*, 377.
- Lewis, W. S.; Cody, V.; Galitsky, N.; Luft, J. R.; Pangborn, W.; Chunduru, S. K.; Spencer, H. T.; Appleman, J. R.; Blakley, R. L. *J. Biol. Chem.* **1995**, *270*, 5057.
- McTigue, M. A.; Davies II, J. F.; Kaufman, B. T.; Kraut, J. *Biochemistry* **1992**, *31*, 7264.
- Champness, J. N.; Achari, A.; Ballantine, S. P.; Bryant, P. K.; Delves, C. J.; Stammers, D. K. *Structure* **1994**, *2*, 915.
- Sali, A.; Blundell, T. L. *J. Mol. Biol.* **1993**, *234*, 779.
- Altschul, S. F.; Gish, W.; Miller, W.; Myers, E. W.; Lipman, D. J. *J. Mol. Biol.* **1990**, *215*, 403.
- Laskowski, R. A.; McArthur, M. W.; Moss, D. S.; Thornton, J. M. *J. Appl. Cryst.* **1993**, *26*, 283.
- Pearlman, D. A.; Case, D. A.; Caldwell, J. W.; Ross, W. S.; Cheatman III, T. E.; Ferguson, D. M.; Kollman, P. A. *AMBER 4.1*. University of California: San Francisco, 1995.
- Cornell, W. D.; Cieplak, P.; Bayly, C. I.; Gould, I. R.; Merz, K. M.; Ferguson, D. M.; Spellmeyer, D. C.; Fox, T.; Caldwell, J. W.; Kollman, P. A. *J. Am. Chem. Soc.* **1995**, *117*, 5179.
- van Gasteren, W. F.; Berendsen, H. J. C. *Mol. Phys.* **1977**, *34*, 1311.
- Penner, M. H.; Frieden, C. *J. Biol. Chem.* **1985**, *260*, 5366.
- Fierke, C. A.; Johnson, K. A.; Benkovics, S. J. *Biochemistry* **1987**, *26*, 4085.
- Appleman, J. R.; Howell, E. E.; Kraut, J.; Blakley, R. L. *J. Biol. Chem.* **1990**, *265*, 5579.
- Costantino, L.; Rastelli, G.; Vescovini, K.; Cignarella, G.; Vianello, P.; Corso, A. D.; Cappiello, M.; Mura, U.; Barlocco, D. *J. Med. Chem.* **1996**, *39*, 4396.
- Bayly, C. I.; Cieplak, P.; Cornell, W. D.; Kollman, P. A. *J. Phys. Chem.* **1993**, *97*, 10269.
- Cieplak, P.; Bayly, C. I.; Cornell, W. D.; Kollman, P. A. *J. Comput. Chem.* **1995**, *16*, 1357.
- Jorgensen, W. L.; Chandrasekhar, J.; Madura, J. D.; Impey, R. W.; Klein, M. L. *J. Chem. Phys.* **1983**, *79*, 926.
- Cocco, L.; Roth, B.; Temple, Jr., C.; Montgomery, J. A.; London, R. E.; Blakley, R. L. *Arch. Biochem. Biophys.* **1983**, *226*, 567.
- Cocco, L.; Groff, J. P.; Temple, Jr., C.; Montgomery, J. A.; London, R. E.; Matwiyoff, N. A.; Blakley, R. L. *Biochemistry* **1981**, *20*, 3972.
- Varnex, A.; Helissen, S.; Wipff, G.; Collet, A. *J. Comput. Chem.* **1998**, *19*, 820.

41. Carrington, H. C.; Crowther, A. F.; Stacey, G. J. *J. Chem. Soc.* **1954**, 1017.
42. Colebrook, L. D.; Giles, H. G.; Rosowsky, A.; Bentz, W. E. *Can. J. Chem.* **1976**, *54*, 3757.
43. Modest, E. J. *J. Org. Chem.* **1956**, *21*, 1.
44. Modest, E. J.; Levine, P. *J. Org. Chem.* **1956**, *21*, 14.
45. Mamalis, P.; Green, J.; Outred, D. J.; Rix, M. *J. Chem. Soc.* **1962**, 3915.
46. Sirawaraporn, W.; Prapunwattana, P.; Sirawaraporn, R.; Yuthavong, Y.; Santi, D. V. *J. Biol. Chem.* **1993**, *268*, 21637.
47. Blakley, R. L.; Benkovics, S. J. In *Folates and Pteridines*; Blakley, R. L.; Benkovics, S. J., Eds.; Wiley: New York, 1984; Vol. 1, pp 191–253.
48. Lemcke, T.; Christensen, I. T.; Jørgensen, F. S. *Bioorg. Med. Chem.* **1999**, *7*, 1003.
49. Smith, D. R.; Calvo, J. M. *Nucleic Acids Res.* **1980**, *8*, 2255.
50. Freisheim, J. H.; Bitar, K. G.; Reddy, A. V.; Blankenship, D. T. *J. Biol. Chem.* **1978**, *253*, 6437.
51. Masters, J. N.; Attardi, G. *Gene* **1983**, *21*, 59.
52. Chen, M.-J.; Shimada, T.; Moulton, A. D.; Cline, A.; Humphries, R. K.; Maizel, J.; Nienhuis, A. W. *J. Biol. Chem.* **1984**, *259*, 3933.
53. Kumar, A. A.; Blankenship, D. T.; Kaufman, B. T.; Freisheim, J. H. *Biochemistry* **1980**, *19*, 667.
54. Edman, J. C.; Edman, U.; Cao, M.; Lundgren, B.; Kovacs, J. A.; Santi, D. V. *Proc. Natl. Acad. Sci. USA* **1989**, *86*, 8625.